THE JOURNAL OF PHYSICAL CHEMISTRY C

Article

pubs.acs.org/JPCC

Photoelectrochemical Responses from Zinc Porphyrin-Silver Nanoparticle Composite Films Fabricated on ITO Electrodes

Ryuji Matsumoto,[†] Hiroaki Yonemura,*[,‡] and Sunao Yamada*[,‡]

[†]Department of Materials Physics and Chemistry, Graduate School of Engineering, Kyushu University, 744 Motooka, Nishi-ku, Fukuoka 819-0395, Japan

[‡]Department of Applied Chemistry, Faculty of Engineering, Kyushu University, 744 Motooka, Nishi-ku, Fukuoka 819-0395, Japan

Supporting Information

ABSTRACT: The fabrication of zinc tetraphenyl porphyrin (ZnTPP)−silver nanoparticle (AgP) composite films on indium−tin-oxide (ITO) electrodes were carried out by the electrostatic layer-by-layer adsorption technique. The degree of immobilization of AgPs on the ITO electrodes could be controlled by changing the immersion time into the aqueous colloidal solution of AgPs. Maximum enhancement in the photocurrent action spectra as well as the fluorescence emission spectra was observed when optimum amounts of AgP were deposited onto the ITO electrode for the photocurrent and the fluorescence measurements, respectively. Effect of AgP on the photocurrent and the fluorescence suggested the effects of enhanced electric fields resulting from the localized surface plasmon resonance on the enhancement of photocurrent and fluorescence signals. The effect of AgP on the lifetime of the singlet excited state of ZnTPP (^{1}ZnTPP*) indicated that the lifetime of ^{1}ZnTPP* becomes shorter at an immersion time of 6 h. The results of the fluorescence lifetime suggested that the difference of effects of AgP on the photocurrent and the fluorescence is most likely ascribed by that the energy-transfer from ^{1}ZnTPP* to surface plasmon due to AgP aggregates is competitive with the photoinduced electron-transfer from ^{1}ZnTPP* to O_2 in the photocurrent measurements.

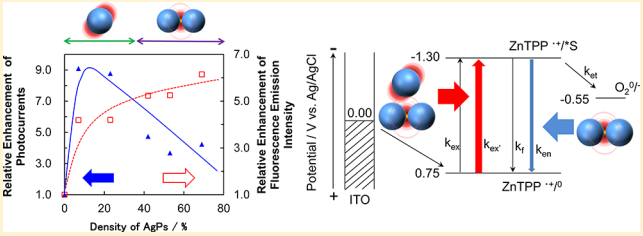

INTRODUCTION

Studies on the photoelectrochemical responses from the excited states of dyes are very important for elucidating the nature of fundamental photochemical reactions such as photoinduced electron-transfer reactions during photosynthesis in biochemical systems.[1] They also provide practical applications such as in the development of organic solar cell,[2] photoelectrochemical biosensing devices,[3] logic gates,[4] and photocatalysis.[5] In the previous studies, photoelectrochemical responses from organic dyes were reported by the combined use of electron donor−acceptor pairs.[6]

Meanwhile, metal nanoparticles (NPs) have been attracting much for their unique optical properties and have been utilized to improve the efficiency of photoelectric conversion[7−30] in solid-state photodiodes,[7−12] photodetecters,[13−15] solar cells,[16−19] and so on. However, in these cases, NPs (or nanoislands) are prepared by vacuum deposition,[11−15,17,18,22−28] lithography,[19−21] or casting of colloidal solution,[7−9,16] thus, controlling the density of the deposited NPs and maintaining size and shape has been difficult. As an alternative approach, we fabricated photovoltaic systems by the self-assembly of an organic dyes either onto a gold nanoparticle (AuP) multistructure that was prepared by a salting-out process,[31] onto the AuP film prepared at the liquid−liquid interface[32] or a electrochemically deposited gold nanostructures.[33] However, those approaches have also a lack of control of the AuP deposition density.

Previously, we reported the technique of electrostatic layer-by-layer adsorption for fabricating multistructures of silver nanoparticles (AgPs).[34] The technique is very convenient and needs no sophisticated equipment such as vacuum systems. Nevertheless, it is easy to control the deposition density of charged NPs by changing the immersion time of the substrate into the corresponding colloidal solution.[35] Recently, we found the remarkable enhancement of photocurrent responses based on the photoexcitation of a tetraphenyl porphyrin or a palladium phthalocyanin derivative as an organic dye adsorbed onto the surfaces of AgPs; the AgP−porphyrin assemblies were prepared by the layer-by-layer technique.[36] However, the detailed mechanism including relationship between the photocurrents and the fluorescence intensities has not yet been elucidated in the organic dye−AgP composite films.

In the present study, we examined the effects of enhanced electric fields resulting from localized surface plasmon resonance (LSPR) on the photocurrents of the zinc tetraphenyl porphyrin (ZnTPP)−AgP composite films and clarified the relationship between the photocurrents or fluorescence intensities of ZnTPP and the amounts of AgP using

Special Issue: Nanostructured-Enhanced Photoenergy Conversion

Received: June 27, 2012
Revised: November 10, 2012
Published: November 13, 2012

ACS Publications © 2012 American Chemical Society

dx.doi.org/10.1021/jp306313w | J. Phys. Chem. C 2013, 117, 2486−2493

fluorescence lifetime measurement to elucidate the mechanism of the effect of LSPR due to AgPs.

EXPERIMENTAL SECTION

Materials. Silver nitrate ($AgNO_3$, Wako), trisodium citrate dehydrate (Wako), poly(ethyleneimine) (PEI, M_w = 50000−100000, Wako), octanethiol (OT, TCI), and other chemicals were used as received. ZnTPP was synthesized in our laboratory. The purity of ZnTPP was confirmed by ^{1}H NMR spectrum.

AgPs were synthesized according to the reported procedure.[34,37] Briefly, $AgNO_3$ (108 mg) was dissolved into H_2O (600 mL). After refluxing, 12 mL of sodium citrate aqueous solution (11 wt %) was injected into the solution and then refluxed for 30 min to produce the AgP colloidal solution. The resultant AgPs were capped with citrate ions, leading to negatively charged surfaces. Extinction spectra of the aqueous solutions of AgP were measured (see Supporting Information, Figure S1). The peak of surface plasmon due to AgP was observed at 403 nm. The average diameter of AgPs was 50 nm, as determined from transmission electron microscope (TEM) images. An indium−tin oxide (ITO) electrode (surface resistivity: 10 Ω/sq, Geomatec Co., Ltd.) was washed with acetone and 2-propanol and then cleaned in an ozone atmosphere for 30 min; this was followed by washing with H_2O and drying with the nitrogen gas before use. Water was deionized with a Milli-Q system (Millipore).

Fabrication of ZnTPP−AgP Composite Films. The ZnTPP−AgP composite films with differing amounts of AgPs were fabricated, modifying the previous method.[36] In this study, we added the step of which self-assembled monolayers (SAMs) of OT were prepared by immersing the ITO-substrate immobilized with AgP in an ethanol solution of OT, because OT is the role of stabilization for photocurrent to avoid the anodic dissolution of the absorbed AgP and/or the oxidation of the absorbed AgP due to O_2. The fabrication procedure of ZnTPP−AgP composite films with different amounts of AgPs is shown in Figure 1. First, the ITO-substrate was immersed into

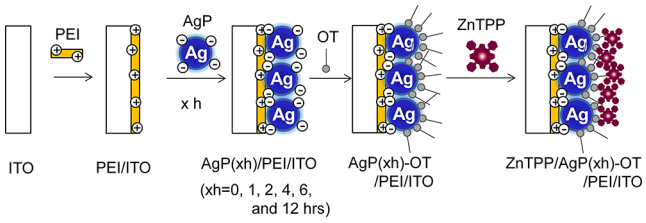

Figure 1. Schematic illustration for the fabrication of zinc tetraphenyl porphyrin (ZnTPP)−AgP composite films on the ITO electrode.

an aqueous PEI solution (3 mM) containing 1 M NaCl for 20 min at 303 K to produce an ITO-substrate modified with PEI. After immersion, the ITO-electrode was washed with H_2O and immersed into H_2O for 20 min; this formed a precursor-modified ITO-electrode denoted as PEI/ITO.[34,38] This positively charged ITO-electrode was then immersed into an aqueous colloidal solution of negatively charged AgPs (AgP(x h)) for different times (x h = 0, 1, 2, 4, 6, 12 h) to immobilize AgPs on the positively charged ITO-electrode by the electrostatic adsorption (denoted as AgP(x h)/PEI/ITO). Next, the SAMs of OT were prepared by immersing AgP(x h)/PEI/ITO in an ethanol solution of OT to stabilize the adsorbed AgP surface, giving the AgP(x h) modified with the SAMs of OT/PEI/ITO, denoted as AgP(x h)-OT/PEI/ITO. Finally, 5 μL of a toluene solution of ZnTPP (0.2 mM) was spin-coated onto the surface of AgP(x h)-OT/PEI/ITO at 1500 rpm and then 2000 rpm for each 10 s by using photoresist spinner (KYOWARIKEN K-359S-1); this gave the ZnTPP-modified AgP(x h)-OT/PEI/ITO, denoted as ZnTPP/AgP(x h)-OT/PEI/ITO. The adsorbed amount of ZnTPP on each substrate was evaluated from absorption spectroscopy. The adsorbed ZnTPP was dissolved with toluene by immersing the ZnTPP-modified AgP(x h)-OT/PEI/ITO into toluene (4 mL) and then by sonicating for 20 min.

Measurements. Extinction spectra were measured on a spectrophotometer (JASCO V-670). TEM images were measured on a TEM (JEOL JEM-2010). Scanning electron microscope (SEM) images were taken on a Hitachi High-Tech SU8000, after drying of the sample under vacuum for over 6 h. Photocurrent measurements were carried out in an aqueous solution containing 0.1 M $NaClO_4$ using the three-electrode photoelectrochemical cell; the three electrodes were modified (working), Ag/AgCl (sat. KCl; reference), and platinum (counter). Before measurements, oxygen bubbling was carried out for 30 min. The monochromatic light from a Xe lamp irradiated the modified electrode, and the resultant photocurrents were measured with a Huso HECS-318C potentiostat. All photocurrents were measured at E = 0 V versus Ag/AgCl.

Steady-state fluorescence emission or excitation spectra were measured on a JASCO FP6500 spectrometer with a photomultiplier (R928 Hamamatsu Photonics Co., Ltd.). Fluorescence emission or excitation spectra of the ZnTPP−AgP composite films were measured using an attachment for the measurements of solid sample (FDA-430 type; JASCO FP6000 series).

In the fluorescence lifetime measurements, a glass was used as a substrate instead of an ITO substrate. AgP(2 or 6 h)-OT/PEI/glass was prepared as described above. Finally, 10 μL of a toluene solution of ZnTPP (10 mM) was casted on the AgP(2 or 6 h)-OT/PEI/glass and glass (denoted as ZnTPP/AgP(2 or 6 h)-OT/PEI/glass and ZnTPP/glass). Fluorescence lifetimes were measured by a single-photon counting system (Hamamatsu Photonics, C4780) using a dye laser (USHO DL-50, 420 nm), a dye (Stilbene 420, Exciton, Inc.), and a N_2 laser (USHO KEN-800).

RESULTS AND DISCUSSION

Characterization of ZnTPP−AgP Composite Films. Characterization of ZnTPP/AgP(x h)-OT/PEI/ITO was carried out by extinction spectra and SEM measurements. The formation of SAMs of OT on the AgP surface was confirmed by the extinction spectra of AgP(x h)/PEI/ITO before and after the immersion of an ethanol solution of OT (see Supporting Information, Figure S2). Namely, the plasmon bands of isolated AgP after the immersion into the OT solution were red-shifted and slightly broadened as compared with those before immersion. The results indicate that the SAMs of OT formed on the AgP surface. Figure 2 shows extinction spectra of ZnTPP/AgP(x h)-OT/PEI/ITO, where x h = 0, 1, 2, 4, 6, and 12 h. The broad absorption band around 400−500 nm is assignable to the plasmon band of isolated AgPs, or the band of transverse oscillation mode of coupled particles; as well as the broad bands around 600−900 nm are assignable to the plasmon band of AgP aggregates in addition to the band for longitudinal oscillation mode of coupled particles, as reported previously.[39] The extinction due to two plasmon bands increased with

dx.doi.org/10.1021/jp306313w | J. Phys. Chem. C 2013, 117, 2486−2493

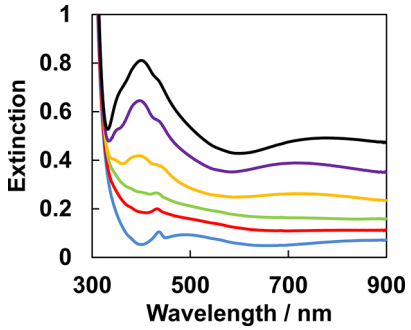

Figure 2. Extinction spectra of ZnTPP/AgP(x h)-OT/PEI/ITO (x = 0, 1, 2, 4, 6, 12), where x h = 0 (blue), 1 (red), 2 (green), 4 (yellow), 6 (purple), and 12 h (black).

increasing the immersion time (x). The latter broad bands were hardly observed in ZnTPP/AgP(1 or 2 h)-OT/PEI/ITO. In contrast, the broad bands appeared clearly in ZnTPP/AgP(4, 6, or 12 h)-OT/PEI/ITO. The results strongly indicate that there are scarcely any AgP aggregates in ZnTPP/AgP(1 or 2 h)-OT/PEI/ITO, while the AgP aggregates exist in ZnTPP/AgP(4, 6, or 12 h)-OT/PEI/ITO.

The plasmon bands of AgP after spin-coating of the toluene solution of ZnTPP were almost same as those before spin-coating. The result indicates that the spin-coating process hardly influences on the nanostructure of adsorbed AgPs in the AgP(x h)-OT/PEI/ITO. On the other hand, a weak absorption band around 430−445 nm is assignable to the Soret band of ZnTPP in ZnTPP/AgP(x h)-OT/PEI/ITO. It is red-shifted as compared with ZnTPP in the toluene solution (423 nm). This may be attributed to the aggregation of ZnTPP in ZnTPP/AgP(x h)-OT/PEI/ITO, and/or the electronic interaction between AgP and ZnTPP, though the precise reason is not confident at this stage.

To evaluate the amount of adsorbed ZnTPP/AgP(x h)-OT/PEI/ITO, we dissolved the adsorbed ZnTPP of ZnTPP/AgP(x h)-OT/PEI/ITO by immersing it into toluene as similar to the previous paper[36] (see Experimental Section). We found the Soret band of ZnTPP in the absorption spectra of ZnTPP-dissolved toluene solution (see Supporting Information, Figure S3). The average amount of adsorbed ZnTPP in ZnTPP/AgP(x h)-OT/PEI/ITO was calculated to be 3.9×10^{13} molecules/cm^2. In spite that the adsorbed amounts of ZnTPP among AgP(x h)-OT/PEI/ITO (x h = 0, 1, 2, 4, 6, and 12 h) were slightly different judging from absorption spectroscopy, the ratio of the adsorbed amounts of ZnTPP in ZnTPP/AgP(x h)-OT/PEI/ITO to ZnTPP/AgP(0 h)-OT/PEI/ITO were estimated to be 0.97−1.12 (see Supporting Information, Table S1).

Figure 3 shows SEM images of AgP(x h)-OT/PEI/ITO (x h = 0, 1, 2, 4, 6, and 12 h), where AgPs are indicated as white spots. It is clear that the number of AgPs increased; at the same time aggregation proceeded as the immersion time (x) into the aqueous colloidal solution increased. The results of the SEM images are in good agreement with those of the extinction spectra (Figure 2). From the SEM images (Figure 3), the density of AgPs in AgP(x h)-OT/PEI/ITO (x h = 1, 2, 4, 6, and 12 h) were estimated to be 7, 23, 46, 53, and 69%, using Image J as free software for image processing and analysis, respectively. The density of AgPs increased with increasing the immersion time (x). These results indicate that the density of

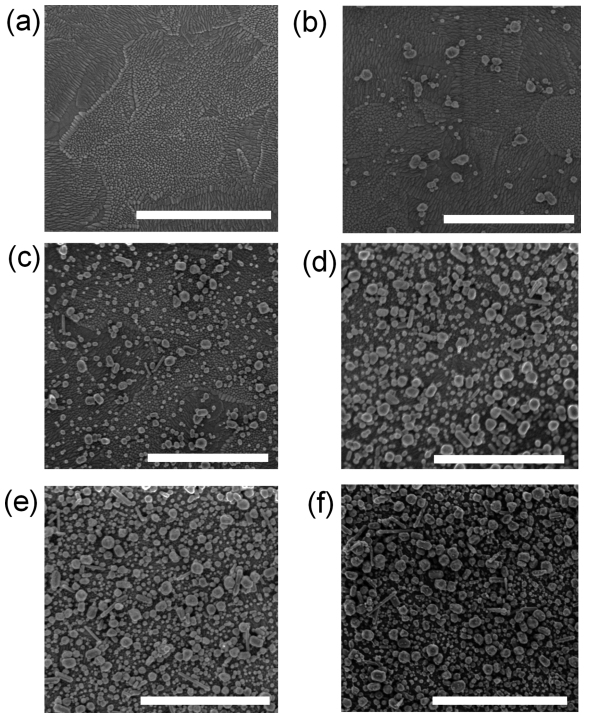

Figure 3. SEM images of AgP(x h)-OT/PEI/ITO (x = 0, 1, 2, 4, 6, 12), where x h = (a) 0, (b) 1, (c) 2, (d) 4, (e) 6, and (f) 12 h (scale bar = 1 μm).

adsorbed AgPs can be controlled by changing the immersion time of the substrate into the colloidal solution.

Photoelectrochemical Measurements of ZnTPP−AgP Composite Films. To investigate the effects of AgP on the photoelectrochemical responses from ZnTPP−AgP composite films, we measured the photocurrent action spectra for all electrodes modified with the ZnTPP−AgP composite films. The results for ZnTPP/AgP(x h)-OT/PEI/ITO (x h = 0, 1, 2, 4, 6, and 12 h) are shown in Figure 4. In all samples,

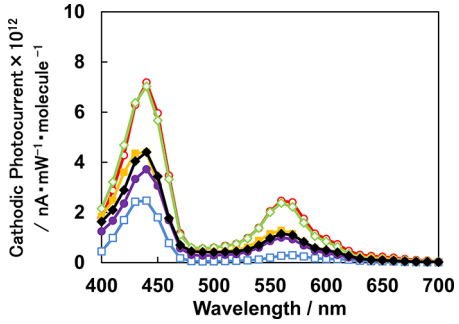

Figure 4. Photocurrent action spectra of ZnTPP/AgP(x h)-OT/PEI/ITO (x = 0, 1, 2, 4, 6, 12), where x h = 0 (blue square), 1 (red circle), 2 (green diamond), 4 (yellow solid square), 6 (purple solid circle), 12 h (black solid diamond).

photocurrents were observed in the cathodic direction. The photocurrent action spectra of all samples were in good agreement with the absorption spectrum of ZnTPP on quartz or in toluene. Therefore, it is suggested that the photocurrents are attributable to the photoexcitation of ZnTPP and subsequent photoinduced electron-transfer to the oxygen in the electrolyte solution. It is noteworthy that the photocurrents in ZnTPP/AgP(x h)-OT/PEI/ITO (x h = 1, 2, 4, 6, and 12 h)

dx.doi.org/10.1021/jp306313w | J. Phys. Chem. C 2013, 117, 2486−2493

are larger than those in ZnTPP/AgP(0 h)-OT/PEI/ITO (Figures 4). In addition, the maximum enhancements of photocurrents at immersion time of 1 or 2 h were observed in the ZnTPP/AgP(1 or 2 h)-OT/PEI/ITO. These enhancements of photocurrents due to AgPs strongly suggest that the local electric fields appearing in the vicinity of AgP surface contribute to the enhancement of photocurrent generation based on the immobilized ZnTPP molecules.

The enhancements of photocurrents due to AgP in the Q-band region (>500 nm) are stronger than those in the Soret band region (400 < λ < 450 nm). These results may be at least due to decrease of irradiation light that can be absorbed by ZnTPP, because isolated AgPs preferentially absorb the incident light around 420 nm (filter effect). Especially, about 9 times relative enhancement of photocurrent at 560 nm in the Q-band region for ZnTPP/AgP(1 and 2 h)-OT/PEI/ITO was observed as compared with the case of ZnTPP/AgP(0 h)/PEI/ITO (Figure 5). On the other hand, about 3 times

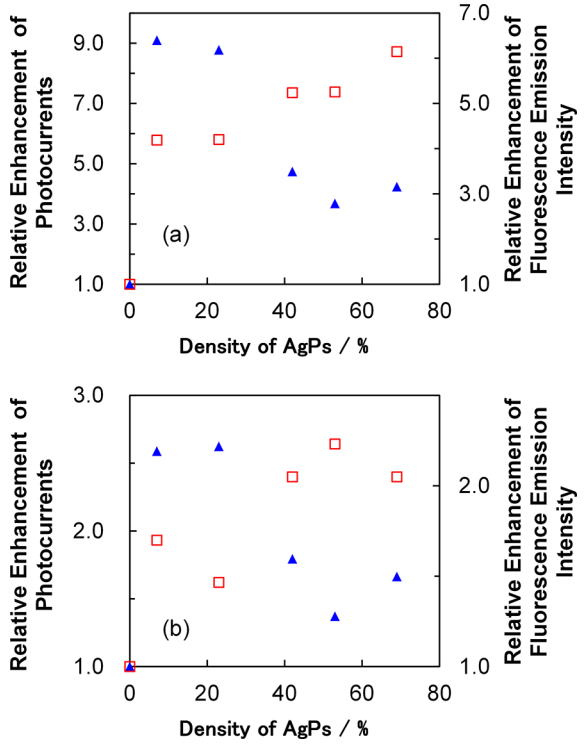

Figure 5. Effect of AgP-density on the relative enhancement of (a) photocurrents at 560 nm (blue solid triangle) and the fluorescence emission intensity at 660 nm (red square) excited at 560 nm, and (b) photocurrents at 430 nm (blue solid triangle) and the fluorescence emission intensity at 660 nm (red square) excited at 430 nm in ZnTPP/AgP(x h)-OT/PEI/ITO (x = 0, 1, 2, 4, 6, and 12).

enhancement of photocurrent at 440 nm in the Soret band region for ZnTPP/AgP(1 and 2 h)-OT/PEI/ITO was observed as compared with the case of ZnTPP/AgP(0h)/PEI/ITO. If the photocurrent from the ZnTPP/AgP(x h)-OT/PEI/ITO (x h = 1, 2, 4, 6, and 12 h) is generated only by simple photoexcitation of immobilized ZnTPP molecules, the photocurrent ratio should be independent of the irradiation wavelength. However, the relative enhancement is dependent on the irradiation wavelength. Therefore, the large enhancement of photocurrents at 560 nm is probably responsible for that surface plasmon of AgP aggregates in addition of the filter effect.[36] The results are similar to those in the photocurrents in the porphyrin/gold nanostructures.[32,33,36]

Effects of AgP-density on the relative enhancement of photocurrents at 560 and 430 nm in ZnTPP/AgP(x h)-OT/PEI/ITO (x h = 1, 2, 4, 6, and 12 h) are shown in Figure 5a,b. The maximum relative enhancements of photocurrents at both 560 and 430 nm were observed in ZnTPP/AgP(1 or 2 h)-OT/PEI/ITO. The maximum relative enhancement (ca. 9 times) of photocurrents at 560 nm was larger than that (ca. 2.6 times) of photocurrents at 430 nm. The large enhancement of photocurrents at 560 nm as compared with that of photocurrents at 430 nm is probably responsible for that surface plasmon of AgP aggregates in addition of the filter effect, as described above. Also, the relative enhancement decreased with increasing the AgP-density in ZnTPP/AgP(4, 6, or 12 h)-OT/PEI/ITO in Figure 5a,b. In addition, the effect of AgP-density on the relative enhancement of photocurrents at 560 nm (Figure 5a) was similar to that of photocurrents at 430 nm (Figure 5b). The result suggests that dependence of AgP-density on photocurrents is independent of the photoirradiation wavelength. However, the effect of AgP-density on the photocurrents in this study is somewhat different from that the relative enhancement of photocurrents tended to saturate up to the density of AgPs (30−50%) in the previous study.[36] The reason is not clear at this stage.

Recently, the similar effect of the density of AuPs on the photocurrents was reported using the electropolymerized polythiophene−AuP composite ITO-electrodes.[40] In the study, the maximum enhancement (ca. 1.5 times) of photocurrents in the presence of AuP (density: 14%) was observed, while the photocurrents (ca. 0.6 times) in the presence of AuP (density: 68%) was smaller as compared with that in the absence of AuP. It is suggested that the decrease of the photocurrents might be attributable to the quenching by AuP in the densely packed condition of AuPs, though the detailed mechanism is not clear. We discussed regarding effects AgP-density on the enhancement of photocurrents as well as fluorescence emission intensity of ZnTPP as described below.

Fluorescence Spectra and Fluorescence Lifetime Measurements of ZnTPP−AgP Composite Films. It has been known that the metal nanoparticles enhance the molecular fluorescence due to the effects of LSPR.[41] We performed the measurements of steady-state fluorescence emission or excitation spectra and fluorescence lifetime of ZnTPP/AgP(x h)-OT/PEI/ITO (x h = 0, 1, 2, 4, 6, and 12 h).

Figure 6a,b show fluorescence emission spectra of ZnTPP/AgP(x h)-OT/PEI/ITO (x h = 1, 2, 4, 6, and 12 h) excited at 430 and 560 nm, where the sample was irradiated from the rear side (from the side of ITO electrode). The fluorescence emission intensity due to ZnTPP excited at both 430 and 560 nm was enhanced in the presence of AgP as compared with that in the absence of AgP. The enhancements of fluorescence emission intensity due to AgP excited at 560 nm (Q-band) are stronger than those excited at 430 nm (Soret band). The dependence of the irradiation wavelength on fluorescence emission intensity showed a similar feature to that of photocurrents (Figure 4). These results strongly suggest that the increase in the adsorbed amount of AgPs leads to a decrease in the incident light at 430 nm for excitation of the strong Soret band region, leading to a decrease in the fluorescence signal of ZnTPP due to the filter effect, as described in the section of photoelectrochemical measurements.

dx.doi.org/10.1021/jp306313w | J. Phys. Chem. C 2013, 117, 2486−2493

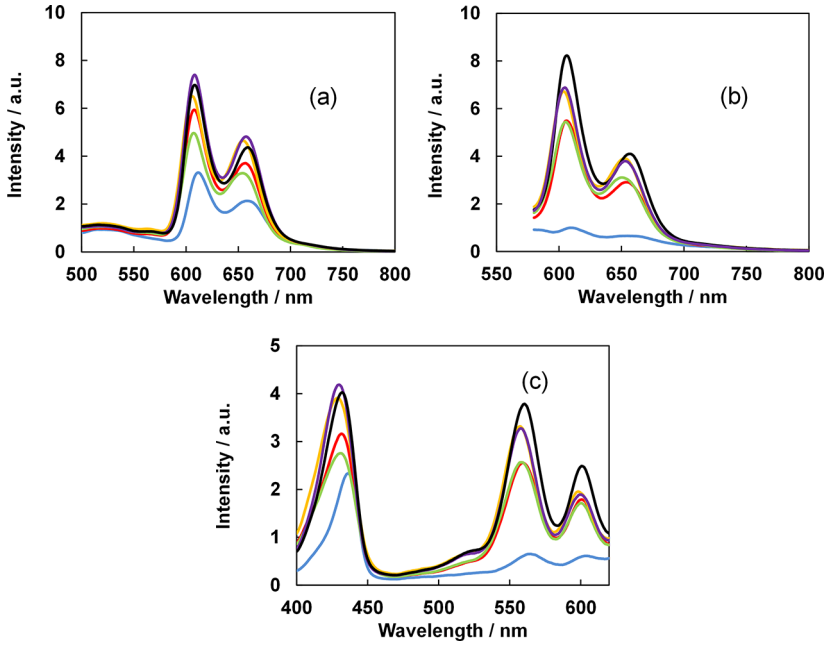

Figure 6. Effects of AgPs on fluorescence emission spectra of ZnTPP/AgP(x h)-OT/PEI/ITO (x = 0, 1, 2, 4, 6, 12) excited at (a) 430 and (b) 560 nm, where x h = 0 (blue), 1 (red), 2 (green), 4 (yellow), 6 (purple), and 12 h (black). (c) Fluorescence excitation spectra of ZnTPP/AgP(x h)-OT/PEI/ITO (x = 0, 1, 2, 4, 6, 12) monitored at 660 nm, where x h = 0 (blue), 1 (red), 2 (green), 4 (yellow), 6 (purple), and 12 h (black).

However, it should be pointed out that ZnTPP in ZnTPP/AgP(x h)-OT/PEI/ITO (x h = 1, 2, 4, 6, and 12 h) showed larger fluorescence signals as compared with the case of ZnTPP/AgP(0 h)-OT/PEI/ITO when the comparison was made under the identical number of ZnTPP, in spite of the presence of the filter effect in ZnTPP/AgP(x h)-OT/PEI/ITO. These results indicate the presence of enhanced excitation of ZnTPP by the localized electric field at the surface region of AgPs.

Figure 6c shows the fluorescence excitation spectra of ZnTPP/AgP(x h)-OT/PEI/ITO (x h = 1, 2, 4, 6, and 12 h) monitored at 660 nm. The peak positions in the photocurrent action spectra of all samples (Figure 4) were in good agreement with the fluorescence excitation spectra (Figure 6c). The results strongly indicate that the photocurrents are attributable to the singlet excited state of ZnTPP (^{1}ZnTPP*). The fluorescence signal at 430 nm increased up to 6 h of immersion time (x h) and then slightly decreased at 12 h. In contrast, the fluorescence signal at 560 nm increased up to 12 h. Effect of immersion time on the fluorescence signal at 430 nm is different from that at 560 nm. The filter effect is probably one of the reasons for the difference described above.

Effects of AgP-density on the relative enhancement of the fluorescence emission intensity at 660 nm excited at 560 and 430 nm in ZnTPP/AgP(x h)-OT/PEI/ITO (x h = 0, 1, 2, 4, 6, and 12 h) are also shown in Figure 5a,b. The fluorescence emission intensities excited at both 560 and 430 nm increase with increasing the AgP-density. It is clear that the effects of AgP-density on the fluorescence emission intensity at 660 nm are clearly different from those on the photocurrents at 560 nm (Figure 5a,b). The maximum relative enhancements of the fluorescence emission intensity at both 560 and 430 nm were observed in ZnTPP/AgP(4 or 6 h)-OT/PEI/ITO. The maximum relative enhancement (ca. 6.1 times) of fluorescence emission intensity excited at Q-band (560 nm) was about 3 times larger than that (ca. 2.2 times) excited at Soret band (430 nm). The enhancement of fluorescence emission intensity excited at Q-band (560 nm) as compared with that excited at Soret band (430 nm) was similar to that of photocurrents at Q-band (560 nm) as compared with that at Soret band (430 nm). The results suggest that the degree of effects of the surface plasmon of AgP aggregates and the filter effect are similar between the photocurrent generation and the fluorescence enhancement. Here, the difference of the effects of AgP-density on between the fluorescence emission intensity and the photocurrents is not attributed to the degree of the filter effect due to the isolated AgPs in the fluorescence spectra and the photocurrent action spectra, because of using the same electrodes in two measurements.

The enhancement of photoproperties (fluorescence emission and photocurrent generation) in Figure 5a,b could be explained by the enhanced electric field generated by LSPR. The enhanced electric field increased with decreasing the interparticle distance of AgPs due to surface plasmon coupling of inter-AgPs. As a consequence, the enhanced electric field increases with increasing the density of AgPs because the interparticle distance of AgPs becomes shorter. The enhancement of photoproperties (fluorescence emission and photocurrent generation) becomes larger with increasing the density of AgPs. The effect of AgP-density on the relative enhancement of the fluorescence emission intensity can be explained by the above consideration. However, in the case of photocurrent generation, the enhancement of photocurrents increased and then decreased with increasing increasing the density of AgPs (Figure 5a,b). It is necessary to elucidate the effect of AgP-density on the relative enhancement of photocurrents. Therefore, we examined fluorescence lifetimes of ZnTPP in ZnTPP−AgP composite films to verify the effect of AgP-density on the relative enhancement of photocurrents.

The fluorescence lifetimes in ZnTPP/AgP(x h)-OT/PEI/glass were measured to investigate the relationship between fluorescence and photocurrent measurements (Table 1). Table

dx.doi.org/10.1021/jp306313w | J. Phys. Chem. C 2013, 117, 2486−2493

Table 1. Fluorescence Lifetimes of ZnTPP in Three Substrates

sample	τ_1 (ns)	τ_2 (ns)	τ_3 (ns)	A_1	A_2	A_3	$\langle\tau\rangle$ (ns)
ZnTPP/glass	3.21	0.51		0.19	0.81		1.02
ZnTPP/AgP(2 h)-OT/PEI/glass	3.21	0.51		0.17	0.83		0.97
ZnTPP/AgP(6 h)-OT/PEI/glass	3.21	0.51	0.14	0.14	0.08	0.9	0.26

1 shows lifetime parameters (τ_1, τ_2, and τ_3 are lifetimes of three components. A_1, A_2, and A_3 are amplitudes of three components. $\langle\tau\rangle$ is amplitude−weighted lifetime).

Fluorescence lifetime measurement is a powerful technique to study the energy and photoinduced electron-transfer mechanisms in molecular systems. The excited state properties of organic dyes can be significantly modified by the proximity of a metal nanostructure through the coupling between surface plasmons and excitons, which may lead to three phenomena: (1) nonradiative metallic quenching, (2) increase in the local excitation field strength, and (3) increase in radiative rate due to plasmon−exciton coupling.[42,43]

Metallic quenching of fluorescent molecules is associated with energy and electron-transfer processes. When the excited molecules are close to the metal surface (typically <5 nm), the excited state of fluorescent molecules can be quenched by the metal via nonradiative Förster-like energy transfer or through electron-transfer between fluorescent molecule and the metal. The second phenomenon increases a local excitation field. The third phenomenon results in faster decay rate of fluorescence. The second and third phenomena give rise to the increase of fluorescence emission intensity.

Thus, the first and third phenomena give rise to a faster decay rate of fluorescence emission of fluorescent molecule, while the second and third phenomena result in increased steady-state fluorescence emission intensity. In addition, a scattering of plasmonic nanostructures which increases the optical path of light in fluorescence materials enhances the light absorption leading to fluorescence enhancement.[30] The far-field effect also increases fluorescence emission intensity without affecting the decay rate, as similar to the second phenomenon (near-field effect).

Thus, the faster radiative decay rate (third phenomenon: plasmon-exciton coupling), increased local excitation field (second phenomenon: surface plasmon resonance (SPR)-enhanced excitation), and scattering which collectively maximize fluorescence emission intensity competes with the metallic quenching (first phenomenon), which suppresses fluorescence emission intensity.

In ZnTPP/AgP(2 and 6 h)-OT/PEI/glass, there are the components of τ_1 (3.21 ns) and τ_2(0.51 ns), which are the same as those in ZnTPP/glass as a reference (Table 1). The results probably indicate that there are some amounts of ZnTPP, which exists far apart in the AgPs, ZnTPP/AgP(2 and 6 h)-OT/PEI/glass, because of the casting method for the immobilization of ZnTPP on the AgP surface.

The $\langle\tau\rangle$-value (0.97 ns) of ZnTPP/AgP(2 h)-OT/PEI/glass was close to that (1.02 ns) of ZnTPP/glass. In contrast, the $\langle\tau\rangle$-value of ZnTPP/AgP(6 h)-OT/PEI/glass (0.26 ns) was smaller than that of glass/ZnTPP. The ZnTPP/AgP(6 h)-OT/PEI/glass results in both increased fluorescence emission intensity and a reduction in fluorescence lifetime, while the ZnTPP/AgP(2 h)-OT/PEI/glass results only in the increased fluorescence emission intensity. The smaller enhancement of photocurrents of the ZnTPP/AgP(6 h)-OT/PEI/ITO as compared with the ZnTPP/AgP(2 h)-OT/PEI/ITO (Figure 4) is probably ascribed to that the lifetime of ^{1}ZnTPP* in ZnTPP/AgP(6 h)-OT/PEI/ITO was smaller than that in ZnTPP/AgP(2 h)-OT/PEI/ITO (Table 1).[44]

The reaction scheme for the photoelectrochemical reactions of ZnTPP/AgP(x h)-OT/PEI/ITO in the presence of AgP is summarized in Figure 7. The relative enhancement of the photocurrents and the fluorescence emission intensities in the ZnTPP/AgP(x h)-OT/PEI/ITO are larger than 1.0 (Figure 5a,b), because of SPR-enhanced excitation (second phenomenon: near-field effect) and the scattering of AgPs (far-field effect) as described above.

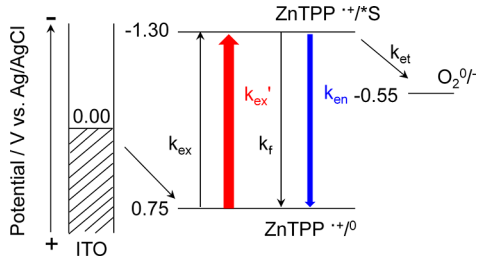

Figure 7. Schematic presentation of reaction scheme of photoelectrochemical reactions in ZnTPP/AgP(x h)-OT/PEI/ITO (x = 1, 2, 4, 6, and 12) in the presence of AgP: k_{et}, rate constant of photoinduced electron-transfer from ^{1}ZnTPP* to O_2; k_{ex}, rate constant of excitation of ZnTPP; k_{ex}', rate constant of excitation of ZnTPP in the presence of AgP (SPR enhanced excitation); k_f, rate constant of fluorescence emission process of ^{1}ZnTPP*; k_{en}, energy transfer from ^{1}ZnTPP* to SP on AgP.

The difference of the effects of AgP-density on the photocurrents and fluorescence emission intensity can be explained in terms of the reaction scheme (Figure 7). The broad plasmon band due to AgP aggregates around 600−900 nm was clearly observed in the ZnTPP/AgP(6 h)-OT/PEI/ITO (Figure 2). The fluorescence emission spectra of ZnTPP (580−700 nm; Figure 6) are superimposed on the plasmon band due to AgP aggregates (600−900 nm) in the ZnTPP/AgP(6 h)-OT/PEI/ITO (Figure 2). Hence, the reduction of fluorescence lifetime in the ZnTPP/AgP(6 h)-OT/PEI/glass is most likely attributable to the energy transfer from ^{1}ZnTPP* to surface plasmon on the AgP aggregates [metallic quenching (first phenomenon) and the plasmon-exciton coupling (third phenomenon)]. Because the lifetime of ^{1}ZnTPP* in the ZnTPP/AgP(6 h)-OT/PEI/glass becomes shorter as compared with that of ZnTPP/glass (Table 1), the energy transfer process of ^{1}ZnTPP* (k_{en}) occurs in the ZnTPP/AgP(6 h)-OT/PEI/ITO (Figure 7). The energy transfer process due to metallic quenching and plasmon-exciton coupling of ^{1}ZnTPP* (k_{en}) is competitive with photoinduced electron-transfer from ^{1}ZnTPP* to O_2 (k_{et}; Figure 7). On the other hand, the broad plasmon band due to AgP aggregates (600−900 nm) was hardly observed in the ZnTPP/AgP(2 h)-OT/PEI/ITO (Figure 2). Therefore, the lifetime of ^{1}ZnTPP* in the ZnTPP/AgP(2 h)-OT/PEI/glass was almost same as of ZnTPP/glass (Table 1). The result indicates that the energy

dx.doi.org/10.1021/jp306313w | J. Phys. Chem. C 2013, 117, 2486−2493

transfer process of ^{1}ZnTPP* (k_{en}) hardly occurs in the ZnTPP/AgP(2 h)-OT/PEI/ITO (Figure 7). On the basis of the above considerations, the photocurrents in ZnTPP/AgP(6 h)-OT/PEI//ITO decreased as compared with that in ZnTPP/AgP(2 h)-OT/PEI//ITO (Figure 5a,b), because the photocurrent is caused by the photoinduced electron-transfer from ^{1}ZnTPP* to O_2 (k_{et}).

Therefore, it is strongly suggested that the photocurrents in ZnTPP/AgP(4, 6, or 12 h)-OT/PEI/ITO was smaller than that in ZnTPP/AgP(1 or 2 h)-OT/PEI/ITO, because the energy transfer process of ^{1}ZnTPP* (k_{en}) occurred in ZnTPP/AgP(4, 6, or 12 h)-OT/PEI/ITO, while that hardly occurred in ZnTPP/AgP(1 or 2 h)-OT/PEI/ITO. The maximum relative enhancement in ZnTPP/AgP(1 or 2 h)-OT/PEI/ITO in the photocurrent generation can be explained by the contribution of the energy transfer process, which is dependent on the AgP-density (Figure 5a,b). In the other words, the results strongly indicate that the energy transfer process, including the plasmon-exciton coupling (third phenomenon), contributes to the reduction of photocurrents in the ZnTPP−AgP composite films.

On the other hand, the plasmon-exciton coupling (third phenomenon) as well as SPR-enhanced excitation (second phenomenon) enhances fluorescence emission intensity of ZnTPP. Therefore, in the case of fluorescence emission measurements, if the plasmon-exciton coupling overcomes the metallic quenching in the energy transfer process of ^{1}ZnTPP* (k_{en}; Figure 7), the fluorescence emission intensity probably increases with increasing the AgP-density, as shown in Figure 5a,b.

The difference in the effect of AgP-density on the photocurrents and fluorescence emission intensity (Figure 5a,b) is most likely explained by the different effects of the plasmon-exciton coupling (third phenomenon) on two behaviors in ZnTPP/AgP(x h)-OT/PEI/ITO (Figure 7).

CONCLUSIONS

In this study, we examined the relationship between the photocurrents or fluorescence due to ZnTPP and the amounts of AgP in the ZnTPP−AgP composite films. The maximum photocurrent of ZnTPP/AgP(1 and 2 h)-OT/PEI/ITO was observed and could be explained by the surface plasmon of the isolated AgP and AgP aggregates and the effects of the isolated AgP and AgP aggregates on the photochemical behaviors of ^{1}ZnTPP*. The results in this study suggest the optimum condition of the amounts of AgP for the photocurrents or the fluorescence of ZnTPP−AgP composite films. Further investigations on the effect of size of AgP on the photocurrents and the fluorescence in the ZnTPP−AgP composite films are now in progress.

ASSOCIATED CONTENT

Supporting Information

Additional figures and table. This material is available free of charge via the Internet at http://pubs.acs.org.

AUTHOR INFORMATION

Corresponding Author

*Tel.: +81-92-802-2814 (H.Y.); +81-92-802-2812 (S.Y.). Fax: +81-92-802-2815 (H.Y.); +81-92-802-2815 (S.Y.). E-mail: yonemura@mail.cstm.kyushu-u.ac.jp (H.Y.); yamada@mail.cstm.kyushu-u.ac.jp (S.Y.).

Notes

The authors declare no competing financial interest.

ACKNOWLEDGMENTS

The authors thank the Center of Advanced Instrumental Analysis, Kyushu University, for performing SEM measurement. The authors are also grateful to Professor Nobuo Kimizuka (Kyushu University) for performing TEM measurements. The present study was financially supported by the Mazda Foundation and by a Grant-in-Aid for Scientific Research: Priority Area of "Strong Photons-Molecules Coupling Fields" (Area 470, No. 19049012), Scientific Research (A; No. 22241028), Scientific Research (C; No. 21550135), and Challenging Exploratory Research (No. 24651145), Nanotechnology Network Project (Kyushu Area Nanotechnology Network), and the Global COE Program "Science for Future Molecular Systems" from MEXT of Japan.

REFERENCES

(1) (a) Das, R.; Kiley, P. J.; Segal, M.; Norville, J.; Yu, A. A.; Wang, L.; Trammell, S. A.; Reddick, L. E.; Kumar, R.; Stellacci, F.; Lebedev, N.; Schnur, J.; Bruce, B. D.; Zhang, S.; Baldo, M. *Nano Lett.* **2004**, *4*, 1079. (b) Frolov, L.; Rosenwaks, Y.; Carmeli, C.; Carmeli, I. *Adv. Mater.* **2005**, *17*, 2434. (c) Lu, Y.; Xu, J.; Liu, Y.; Liu, B.; Xu, C.; Zhao, D.; Kong, J. *Chem. Commun.* **2006**, 785.

(2) (a) O'Regan, B.; Grätzel, M. *Nature* **1991**, *353*, 737. (b) Obermeyer, P.; Haase, C.; Stiebig, H. *Appl. Phys. Lett.* **2008**, *92*, 181102.

(3) (a) Ogasawara, S.; Ikeda, A.; Kikuchi, J. *Chem. Mater.* **2006**, *18*, 5982. (b) Okamoto, A.; Kamei, T.; Saito, I. *J. Am. Chem. Soc.* **2006**, *128*, 658. (c) Liang, M.; Liu, S.; Wei, M.; Guo, L.-H. *Anal. Chem.* **2006**, *78*, 621.

(4) (a) Nitahara, S.; Akiyama, T.; Inoue, S.; Yamada, S. *J. Phys. Chem. B* **2005**, *109*, 3944. (b) Matsui, J.; Mitsuishi, M.; Aoki, A.; Miyashita, T. *Angew. Chem., Int. Ed.* **2003**, *42*, 2272. (c) Gill, R.; Patolsky, F.; Katz, E.; Willner, I. *Angew. Chem., Int. Ed.* **2005**, *44*, 4554.

(5) (a) Fujishima, A.; Honda, K. *Nature* **1972**, *238*, 37. (b) Emeline, A. V.; Furubayashi, Y.; Zhang, X.; Jin, M.; Murakami, T.; Fujishima, A. *J. Phys. Chem. B* **2005**, *109*, 24441. (c) Izawa, K.; Yamada, T.; Unal, U.; Ida, S.; Altuntasoglu, O.; Koinuma, M.; Matsumoto, Y. *J. Phys. Chem. B* **2006**, *110*, 4645.

(6) (a) Yamada, S.; Kohrogi, H.; Matsuo, T. *Chem. Lett.* **1995**, *24*, 639. (b) Dreuw, A.; Worth, G. A.; Cederbaum, L. S.; Head-Gordon, M. *J. Phys. Chem. B* **2004**, *108*, 19049. (c) Luo, C.; Guldi, D. M.; Imahori, H.; Tamaki, K.; Sakata, Y. *J. Am. Chem. Soc.* **2000**, *122*, 6535. (d) Terasaki, N.; Akiyama, T.; Yamada, S. *Langmuir* **2002**, *18*, 8666. (e) Tahara, H.; Yonemura, H.; Harada, S.; Yamada, S. *Jpn. J. Appl. Phys.* **2011**, *50*, 081605. (f) Yonemura, H.; Tahara, H.; Ohishi, K.; Iida, S.; Yamada, S. *Jpn. J. Appl. Phys.* **2010**, *49*, 01AD04.

(7) Schaadt, D. M; Feng, B.; Yu, E. T. *Appl. Phys. Lett.* **2005**, *86*, 063106.

(8) Sundararajan, S. P.; Grady, N. K.; Mirin, N.; Halas, N. J. *Nano Lett.* **2008**, *8*, 624.

(9) Lim, S. H.; Mar, W.; Matheu, P.; Derkacs, D.; Yu, E. T. *J. Appl. Phys.* **2007**, *101*, 104309.

(10) Konda, R. B.; Mundle, R.; Mustafa, H.; Bamiduro, O.; Pradhan, A. K.; Roy, U. N.; Cui, Y.; Burger, A. *Appl. Phys. Lett.* **2007**, *91*, 191111.

(11) Kwon, M.-K.; Kim, J.-Y.; Kim, B.-H.; Park, I.-K.; Cho, C.-Y.; Byeon, C. C.; Park, S.-J. *Adv. Mater.* **2008**, *20*, 1253.

(12) Pillai, S.; Catchpole, K. R.; Trupke, T.; Zhang, G.; Zhao, J.; Green, M. A. *Appl. Phys. Lett.* **2006**, *88*, 161102.

(13) Stuart, H. R.; Hall, D. G. *Appl. Phys. Lett.* **1998**, *73*, 3815.

(14) Collin, S.; Pardo, F.; Pelouard, J.-L. *Appl. Phys. Lett.* **2003**, *83*, 1521.

(15) Tang, L.; Miller, D. A. B.; Okyay, A. K.; Matteo, J. A.; Yuen, Y.; Saraswat, K. C.; Hesselink, L. *Opt. Lett.* **2006**, *31*, 1519.

(16) Derkacs, D.; Lim, S. H.; Matheu, P.; Mar, W.; Yu, E. T. *Appl. Phys. Lett.* **2006**, *89*, 093103.
(17) Pillai, S.; Catchpole, K. R.; Trupke, T.; Green, M. A. *J. Appl. Phys.* **2007**, *101*, 093105.
(18) Stuart, H. R.; Hall, D. G. *Appl. Phys. Lett.* **1996**, *69*, 2327.
(19) Hägglund, C.; Zäch, M.; Petersson, G.; Kasemo, B. *Appl. Phys. Lett.* **2008**, *92*, 053110.
(20) Reilly, T. H.; Lagemaat, J.; Tenent, R. C.; Morfa, A. J.; Rowlen, K. L. *Appl. Phys. Lett.* **2008**, *92*, 243304.
(21) Tvingstedt, K.; Persson, N.-K.; Inganäs, O. *Appl. Phys. Lett.* **2007**, *91*, 113514.
(22) Stenzel, O.; Stendal, A.; Voigtsberger, K.; Borczyskowski, C. *Sol. Energy Mater. Sol. Cells* **1995**, *37*, 337.
(23) Wen, C.; Ishikawa, K.; Kishima, M.; Yamada, K. *Sol. Energy Mater. Sol. Cells* **2000**, *61*, 339.
(24) Westphalen, M.; Kreibig, U.; Rostalski, J.; Lüth, H.; Meissner, D. *Sol. Energy Mater. Sol. Cells* **2000**, *61*, 97.
(25) Uemura, S.; Yoshida, M.; Kodzasa, T.; Yase, K.; Kamata, T. *Synth. Mater.* **2003**, *137*, 1443.
(26) Ishikawa, K.; Wen, C.-J.; Yamada, K.; Okubo, T. *J. Chem. Eng. Jpn.* **2004**, *37*, 645.
(27) Rand, B. P.; Peumans, P.; Forrest, S. R. *J. Appl. Phys.* **2004**, *96*, 7519.
(28) Morfa, A. J.; Rowlen, K. L.; Reilly, T. H.; Romero, M. J.; van de Lagemaat, J. *Appl. Phys. Lett.* **2008**, *92*, 013504.
(29) Kim, S.-S.; Na, S.-I.; Jo, J.; Kim, D.-Y.; Nah, Y.-C. *Appl. Phys. Lett.* **2008**, *93*, 073307.
(30) Atwater, H. A.; Polman, A. *Nat. Mater.* **2010**, *9*, 205.
(31) (a) Kuwahara, Y.; Akiyama, T.; Yamada, S. *Langmuir* **2001**, *17*, 5714. (b) Akiyama, T.; Inoue, K.; Kuwahara, Y.; Terasaki, N.; Niidome, Y.; Yamada, S. *J. Electroanal. Chem.* **2003**, *550*−*551*, 303. (c) Akiyama, T.; Inoue, K.; Kuwahara, Y.; Niidome, Y.; Terasaki, N.; Nitahara, S.; Yamada, S. *Langmuir* **2005**, *21*, 793.
(32) Akiyama, T.; Nakada, M.; Terasaki, N.; Yamada, S. *Chem. Commun.* **2006**, 395.
(33) Akiyama, T.; Aiba, K.; Hoashi, K.; Wang, M.; Sugawa, K.; Yamada, S. *Chem. Commun.* **2010**, *46*, 306.
(34) (a) Arakawa, T.; Akiyama, T.; Yamada, S. *Trans. Mater. Res. Soc. Jpn.* **2008**, *33*, 185. (b) You, J.; Arakawa, T.; Munaoka, T.; Akiyama, T.; Takahashi, Y.; Yamada, S. *Jpn. J. Appl. Phys.* **2011**, *50*, 04DK22(1−4). (c) You, J.; Takahashi, Y.; Yonemura, H.; Akiyama, T.; Yamada, S. *Jpn. J. Appl. Phys.* **2012**, *51*, 02BK04(1−4).
(35) (a) Gole, A.; Sainkar, S. R.; Sastry, M. *Chem. Mater.* **2000**, *12*, 1234. (b) Yonezawa, T.; Onoue, S.; Kunitake, T. *Adv. Mater.* **1998**, *10*, 414.
(36) Arakawa, T.; Munaoka, T.; Akiyama, T.; Yamada, S. *J. Phys. Chem. C* **2009**, *113*, 11830.
(37) Lee, P. C.; Meisel, D. *J. Phys. Chem.* **1982**, *86*, 3391.
(38) Schmitt, J.; Decher, G.; Dressick, W. J.; Brandow, S. L.; Geer, R. E.; Shashidhar, R.; Calvert, J. M. *Adv. Mater.* **1997**, *9*, 61.
(39) Goulet, P. J. G.; dos Santos, D. S.; Alvarez-Puebla, R. A.; Oliveira, O. N.; Aroca, R. F. *Langmuir* **2005**, *21*, 5576.
(40) Takahashi, Y.; Taura, S.; Akiyama, T.; Yamada, S. *Langmuir* **2012**, *28*, 9155.
(41) (a) Kulakovich, O.; Strekal, N.; Yaroshevich, A.; Maskevich, S.; Gaponenko, S.; Nabiev, I.; Woggon, U.; Artemyev, M. *Nano Lett.* **2002**, *2*, 1449. (b) Akiyama, T.; Kawahara, T.; Arakawa, T.; Yamada, S. *Jpn. J. Appl. Phys.* **2008**, *47*, 3063. (c) Tanaka, H.; Mitsuishi, M.; Miyashita, T. *Chem. Lett.* **2005**, *34*, 1246.
(42) (a) Lakowicz, J. R. *Anal. Biochem.* **2001**, *298*, 1. (b) Geddes, C. D.; Lakowicz, J. R. *J. Fluoresc.* **2002**, *12*, 121.
(43) Chen, Y.; Munechika, K.; Jen-La Plante, I.; Munro, A. M.; Skrabalak, S. E.; Xia, Y.; Ginger, D. S. *Appl. Phys. Lett.* **2008**, *93*, 053106.
(44) Aslan, K.; Lakowicz, J. R.; Geddes, C. D. *Anal. Bioanal. Chem.* **2005**, *382*, 926.